INVERSION OF TRAVEL TIME FOR VELOCITY USING MULTI-SPACING SONIC TOOLS

by

Benoit J. Paternoster

Earth Resources Laboratory
Department of Earth, Atmospheric, and Planetary Sciences
Massachusetts Institute of Technology
Cambridge, MA 02139

ABSTRACT

Spatial resolution of sonic logs is greatly affected by the minimum spacing between receivers. Improvements can be made, however, when the spatial sampling of the formation is less than the minimum spacing. This paper proposes a recursive least squares inversion of travel times based on the Kalman filter. This formulation emphasizes the noise content of the data as a factor limiting resolution. Synthetic data as well as real data processing is presented here.

INTRODUCTION

In full waveform acoustic logging, the general trend has been to increase the source to receiver separation as well as the receiver spacing, in order to obtain a deeper penetration of the unperturbed formation and to measure velocity more accurately. The increases of the spacing between receivers and the length of the receiver array have the undesirable effect of smoothing out the variation of velocities over short depth increments. This could cause reduction in spatial resolution, especially in cases where thinly layered stratigraphic units are present. In this study we introduce a method to help resolve the velocities and thicknesses of the thin beds.

Willis (1983) introduced a least squares inversion scheme to determine the transit times and velocities for individual beds. This inversion method is relatively slow and can become cumbersome when applied to large sections. We propose a stochastic formulation that enables us to recursively solve for the transit times. This procedure amounts to removing the effect of the tool length, which acts as a running sum filter. It can also be viewed as a deconvolution process of the tool response. In the following sections we describe the method and its applications to synthetic as well as real data.

FORWARD PROBLEM

The arrival time of acoustic waves is a function of the borehole radius, the velocity of compressional waves in the fluid and the formation body waves, as well as the length of the tool.

Nevertheless, in a first order approximation such as we assume valid for this paper, one can simply relate the arrival time of a given wave, its transit time as a function of depth, and the length of the tool :

$$T(Z) = \frac{1}{Sp} \int_{Z-Sp}^{Z} t(z)dz \tag{1}$$

where Sp is the source receiver separation, $t(z)$ is the formation transit time at depth z, while $T(Z)$ is the arrival time at depth Z per unit length, assuming that source and receiver are located at depth Z and $Z - Sp$. With this formula, delays due to propagation in the fluid are neglected. However, for clarity's sake the formulation presented next is expressed in terms of travel times. Similar developments could be made in terms of moveouts between common source or common receiver pairs.

As seen in Figure 1, a sharp interface would appear, basically, as a ramp of the tool length, and a thin layer would be spatially "diluted" so that its exact location, as well as its "true" transit time, would be hard to resolve. There is a need for improving the spacial resolution of acoustic logs.

Following Foster et al. (1952), we believe that a finer resolution can be gained from logs where measurements are repeated at every fraction of the source receiver separation. In this case the problem can be set in a straightforward manner using the discrete depth version of equation (1):

$$T_j = \frac{1}{N} \sum_{i=j-N+1}^{j} t_i \tag{2}$$

In this equation, discrete depth intervals are taken to be the fraction of the tool length by which it is shifted between successive shots. N is the number of discrete depth intervals over which the loop stretches. Again, t_i is the transit time of the i^{th} depth interval and T_j the arrival time scaled to one discrete depth interval when the top of the tool is at depth j. Depth indices start downhole.

SINGLE SPACING TRAVEL TIME INVERSION

Straightforward least squares inversion

When the tool is run from depth 0 up to depth n, we can set a linear system of equations such as :

$$N.T_0 = t_{1-N} + t_{2-N} + \cdots \qquad \cdots + t_{-2} + t_{-1} + t_0$$

$$N.T_1 = t_{2-N} + t_{3-N} + \cdots \qquad \cdots + t_{-1} + t_0 + t_1$$

$$N.T_N = t_1 + t_2 + \cdots \qquad \cdots + t_{N-2} + t_{N-1} + t_N$$

$$N.T_n = t_{n-N+1} + t_{n-N+2} + \cdots \qquad \cdots + t_{n-2} + t_{n-1} + t_n$$

The redundancy we want to use appears in this system of equations. Except for the N first and N last t_j's, each t_j appears N times in the system. This system has $n+N$ unknowns and n equations. Inverse theory suggests a method for treating such a problem using least squares. This would do well in noise corrupted situations by finding the "best" fit of t_j's for the observation T_j's. Inverting the whole system is, basically, the solution proposed by Willis (1983).

If we are to invert for a large section of the formation, this inversion scheme requires, unfortunately, the handling of large matrices. Moreover, assuming that the problem has been solved for the first n depths, the question is whether the whole system should be inverted again if we add one extra observation ?

Recursive least squares inversion formulation

[1] Up to this point, we have kept the discussion general. Let us take our problem a step further.

A simple look at any section of sonic logs, or at any section of real earth material, will convince us of the vertical sequentiality of the physical characteristics in the earth. More sophisticated evidence of this important geological feature is given by O'Doherty and Anstey (1971). The fact that auto-correlations of reflection coefficient series do not reduce a single spike clearly demonstrates that:

> "the earth stratification is the result of natural laws, that these provide some predictable constraints, and that, consequently, the outcome is not completely random".

How shall we transform this piece of knowledge into analytical constraints for our inversion problem?

First of all, we recast the whole problem in the light of a stochastic process. From now on, the transit times and the arrival times will be considered as random variables. Their depth series can be viewed as stochastic processes. We chose an independent increment process to represent the behavior of the depth sequence of the t_j's. That is,

$$t_{j+1} = t_j + w_j \tag{3}$$

In this equation, w_j is assumed to be a zero mean white noise process independent of t_j. Testing on real and synthetic data has shown that acceptable results can be obtained with equation (3). The "noise" denomination should not mislead the reader. w_j represents the "innovation" of the formation or its departure from a homogeneous formation. It is characterized by a variance q_j. This variance is a measure of the variability of the formation or of the confidence we have in equation (3). Large variances (several orders of magnitude larger than the measurement error variance) will denote that there is very little confidence in the equation. On the other hand, small variances denote that little variation is expected in the formation. Finally, we understand that q_j represents an "a priori" knowledge we may have of the formation and how it can be weighted gradually.

[2] At this point, let us perform some formal changes which will not affect the generality of our discussion :

$$\text{Let} \quad \bar{t}_j = \begin{bmatrix} t_j \\ \cdot \\ \cdot \\ t_{j-N+1} \end{bmatrix} , \quad h = \begin{bmatrix} 1/N \\ 1/N \\ \cdot \\ 1/N \end{bmatrix} \quad \text{and} \quad F = \begin{bmatrix} 1 & 0 & 0 & 0 \\ 1 & 0 & 0 & 0 \\ 0 & 1 & \cdots & \cdots \\ \cdots & \cdots & 0 & 0 \\ 0 & 0 & 1 & 0 \end{bmatrix}$$

Then, our transit time depth sequence is ruled by :

$$\bar{t}_j = F\,\bar{t}_{j-1} + \bar{w}_j \tag{4}$$

The original system of equations can be re-created by successive :

$$T_j = h^T \bar{t}_j + v_j \tag{5}$$

where h^T is the transpose of matrix h. Here, we allowed each travel time observation to be corrupted by a white noise of covariance R_j, representative of the reading error. The covariance matrix, $Q_j = E[\bar{w}_j \bar{w}_j^T]$ characterizes $\bar{w}_j$. Its only non zero entry is the first one in the first row: q_j.

Our present specific problem is to estimate, or invert, for n successive values of $\bar{t}_j$ given n successive measurements or observations T_j related to the $\bar{t}_j$'s through equation (5), under the n linear constraints of consecutive equations (4). In addition to its better constrained nature, the structure of this problem yields estimate computations that can be organized conveniently in a recursive algorithm. This is the Kalman filter.

[3] The remainder of this section will be devoted to the Kalman model formulation. The adequacy of that model for our present purposes can be easily checked. We shall use similar notations.

Two equations define the model :

$$\bar{t}_j = F(j)\,\bar{t}_{j-1} + G(j)\,\bar{w}_j \tag{6}$$

$$\bar{T}_j = H(j)\,\bar{t}_j + \bar{v}_j \tag{7}$$

Equation (6) represents the time dependent behavior of a linear dynamic system. The system is completely characterized by its state vector $\bar{t}_j$. It is also driven by the input $\bar{w}_j$ which, in this application, is a white noise of covariance Q_j. This matrix expresses the confidence we have in this finite difference equation. Following Control Theory terminology, this equation, as well as its counterpart in our present problem, equation (4), will be referred to as the **State equation.**

We perceive the dynamic system only through periodic measurements. The vector of observations, $\bar{T}_j$, is related to the state vector via the linear equation (7). Moreover, the measurement is corrupted by a white noise $\bar{v}_j$ of covariance R_j. R_j is related to the confidence we have in those measurements. This equation will be referred to as the **Measurement** or **observation equation.**

As for any linear system described by a recursive equation, the initial state has to be known. Here, it is specified through the mean and covariance of $\bar{t}_0$. Additional assumptions regarding the independence of the various stochastic processes are to be made. Namely, the noises $\bar{v}_j$ and $\bar{w}_j$ are to be independent of $\bar{t}_0$. Moreover, at a given time both noises are uncorrelated and each, taken at two different times, presents values that are uncorrelated. Figure 2 summarizes the different filter inputs.

[4] The estimate of $\bar{t}_j$, $\hat{t}_j$ which minimizes the error covariance $E[(\hat{t}_j - \bar{t}_j)(\hat{t}_j - \bar{t}_j)^T]$, is $E[\bar{t}_j \mid \bar{T}_j, \ldots, \bar{T}_0]$, the conditional expectation of $\bar{t}_j$ given all past and present observations. This estimate is a linear function of the observations when all random variables are Gaussian. However, when this is not valid (probably our case), the linear function obtained in the Gaussian case still yields the minimum of the error covariance in the set of all possible linear estimators. This is the linear least squares estimator. In the following, $E[X \mid Y]$ is used as the linear least squares estimator of X given Y.

Given the model and the assumptions described in section [3], the problem solved by Kalman is to provide $\hat{t}_j$, the linear least squares estimate of $\bar{t}_j$ given the measurements $\bar{T}_0$ through $\bar{T}_j$. Basically both the estimate $\hat{t}_j$ and its error covariance are propagated in time through a two step recursion. We first define some notations to differentiate between the two steps :

$$\hat{t}(j \mid j-1) = E[\bar{t}_j \mid \bar{T}_{j-1}, \ldots, \bar{T}_0]$$

and $$P(j \mid j-1) = E[\,(\,\bar{t}_j - \hat{t}(j \mid j-1)\,)\,(\,\bar{t}_j - \hat{t}(j \mid j-1)\,)^T\,]$$

$$\hat{t}_j = \hat{t}(j \mid j) = E[\bar{t}_j \mid \bar{T}_j, \bar{T}_{j-1}, \ldots, \bar{T}_0]$$

and $$P(j \mid j) = E[\,(\,\bar{t}_j - \hat{t}(j \mid j)\,)\,(\,\bar{t}_j - \hat{t}(j \mid j)\,)^T\,]$$

The state equation is fruitfully employed to propagate the estimate from time $j-1$ to the next time increment using the same set of observations. Thus a prediction of $\hat{t}_j$ is made: $\hat{t}(j/j-1)$. The estimate of t_j is based on $t(j-1)$. The measurement at time j then adds a new piece of information that is decomposed into a predictable part and an innovative part, which helps correct the prediction through a gain factor $K(j)$. For the sake of clarity we omitted the possible time dependence for the matrices F, G and H. The recursion is as follows:

Step (0) : initialization

$\hat{t}(0\,|\,-1)$: guess of the initial "true" transit times

$P(0\,|\,-1)$: confidence we have in that guess.

Step (1) : correction

$$\hat{t}(j\,|\,j) = \hat{t}(j\,|\,j-1) + K(j)\nu(j);$$

$$P(j\,|\,j) = P(j\,|\,j-1) - K(j)\;H\;P(j\,|\,j-1);$$

$$K(j) = P(j\,|\,j-1)\;H^T[H\;P(j\,|\,j-1)\;H^T + R_j]^{-1};$$

$$\nu(j) = \overline{T}_j - H\,\hat{t}(j\,|\,j-1).$$

Step (2) : prediction

$$\hat{t}(j\,|\,j-1) = F\;\hat{t}(j-1\,|\,j-1);$$

$$P(j\,|\,j-1) = F\;P(j-1\,|\,j-1)\;F^T + G\;Q_j\;G^T.$$

These equations can be directly programmed with the matrices defined in [2] to solve our problem, since our main interest lies in multiple source/receiver combinations.

MULTIPLE SPACINGS TRAVEL TIME INVERSION FORMULATION

Extension to multiple spacings

Sections [1] and [2] of the previous part showed how we could bring our inversion problem in the case of a single spacing tool to a somewhat improved constrained problem. Sections [3] and [4] presented the formulation in a more general situation, in particular that of multiple observations. This showed that our inversion could easily be extended to multi-source, multi-receiver tools. To do that we only have to arrange equation (5) of section [2] where the T_j's become column vectors with as many entries as off-sets to be considered, and h has to be turned into a matrix according to the tool configuration. Assuming it has an integral value, N will be equal to the length of the largest source receiver separation divided by the change in depth of the tool between two completed firing sequences.

Although formation variability and noise covariances can be depth dependent, we kept them at a constant value throughout subsequent applications, in order to simplify the problem and aid in the understanding of the process.

To use this inversion scheme we had to choose a tool configuration. We modelled the case of a two source/two receiver tool such as the one shown in Figure 3. Two sources are placed 2 ft apart at the bottom of the sonde, and two receivers are placed 2 ft apart at the top of the sonde. The distance between the lower receiver and the upper source is 8 ft. This configuration provides source-receiver separations of 8, 10, 10 and 12 ft for each firing sequence. We also assumed in all examples that a complete sequence of shots was fired at 1/2 ft intervals.

Least squares processing

With these specifications our state vector $\bar{t}_j$ has 24 entries. H is a 4 by 24 matrix to accommodate four measurements at every depth increment. The observation equation (5) becomes :

$$\bar{T}_j = H\bar{t}_j + \bar{v}$$

$$\bar{T}_j = \begin{bmatrix} T_j(10) \\ T_j(8) \\ T_j(12) \\ T_j(10) \end{bmatrix};$$

$$H = \begin{bmatrix} 1/20 & 1/20 & 1/20 & 1/20 & 1/20 & .. & 1/20 & 0 & 0 & 0 & 0 \\ 0 & 0 & 0 & 0 & 1/16 & .. & 1/16 & 0 & 0 & 0 & 0 \\ 1/24 & 1/24 & 1/24 & 1/24 & 1/24 & .. & 1/24 & 1/24 & 1/24 & 1/24 & 1/24 \\ 0 & 0 & 0 & 0 & 1/20 & .. & 1/20 & 1/20 & 1/20 & 1/20 & 1/20 \end{bmatrix}$$

We remember that our Kalman filter provides us with vector estimates of $\bar{t}_j$. The scalar function of depth estimates presented next will be the last entry of each state vector estimate. This means that we "wait" until the tool has been completely pulled above the corresponding depth before keeping the estimate. In other words, in order to estimate the formation's "true" transit times, we use the maximum of observations this formulation permits. Formally, the selected estimate will be :

$$E[t_j \mid \bar{T}_{j+N-1}, \ldots, \bar{T}_j, \ldots, \bar{T}_0]$$

Conventional processing

A conventional processing of the arrival times from all four source-receiver combinations could :

(1) Consider all four possible common source and common receiver combinations and compute the Δt's corresponding to 2 ft intervals.

(2) Refer each Δt to the middle 1/2 ft layers in the 2 ft interval.

(3) Average all Δt's corresponding to the same 1/2 ft layer.

Note that in this case, each transit time determination will involve only 8 travel time measurements. We also expect the resolution of such processing to be limited to the smallest spacing, no matter how densely the formation is sampled. We are now ready to try both processes on synthetic travel time data.

SYNTHETIC RESULTS

Noise free situation

Figure 4 displays synthetic arrival time curves versus depth for the four source-receiver combinations in a sharp interface case. The time scale is arbitrary since all arrival times have been scaled to a unique reference length. All transit time estimations will be scaled to that same reference length in order to ease comparisons. A number of discrete depth intervals of 1/2 ft have been plotted on the horizontal axis.

The four curves have been processed by both the conventional and recursive least squares methods. Outputs from both methods are shown in Figure 5.

The conventional processing has an effective resolution equal to the smallest source or receiver separation while the least squares processing inverts exactly for the transit time model discretized every 1/2 ft when input parameters Q and R specify that very little noise is expected in the data.

Noise corrupted situation

We corrupted the arrival time data of Figure 4 with a random additive perturbation having a maximum amplitude of 20 arbitrary units. In the resulting data set, shown in Figure 6, arrival time curves are indistinguishable one from another.

The least squares inversion scheme was tried first. In Figure 7A we kept the input parameter R at a constant value of 20, and increased parameter Q, which describes the formation variability, from a value of 0.1 up to a value of 300, ending with the dashed curve. The filter response to the step change in transit times varies from a slow and smooth change to a quick but noisy rise. Next, in Figure 7B, we started from the last Q and R specifications that yielded the dashed curve and progressively increased R, the observation noise variance, from a value of 20 up to 1000. The filtered output deformed back to a slow rising and smooth curve.

From Figure 7 it appears that the result of the least squares inversion depends greatly on the ratio of expected formation variability to expected noise variance in the data (Q/R ratio). This factor is very similar to that of a damping factor in a damped least squares inversion.

For a high Q/R ratio, the result is mainly affected by the noise content of the data. No "a priori" knowledge of the formation is input and there is even some expectation of large variability. The filter gives more weight to the data and merely uses the state equation. It responds quickly to the step input but shows a high noise content. This is the *quick Kalman filter* case.

For a small Q/R ratio, the result is a very smoothed version of the original model. One does input the "a priori" knowledge. Given that the formation velocity is V at depth i, it is very unlikely that a much smaller or greater velocity than V comes up at depth $i+1$. The filter gives more weight to the state equation and smoothes out the noise. The noise content is small, the resolution poor. This is the *slow Kalman filter* case.

These considerations suggest a trade-off between noise reduction and resolution. The filter will determine a real variation in the transit times we invert for only if the variations in the data set are *more likely* to be due to formation variability (given specification of Q) than to noise corruption (given R).

Figure 8 compares results of the conventional processing for that same noise corrupted data set with those of a quick Kalman filter case (note the slight change of scale from previous figures). The two are very similar. In other words, they depend greatly on the noise content of the data set. This suggests that, in terms of noise reduction, it is possible to do better with the help of some "a priori" knowledge than one can with conventional processing. Both cases have good spatial resolution of the sharp interface, but include variations that do not exist. A slower Kalman filter would not show any variation, unless given likely state/noise variance specifications.

In all results presented here, we have kept R and Q constant. Nevertheless, it must be remembered that this was not a limitation of the method, only a choice made for the sake of greater simplicity. We could have varied R and Q values in the course of the algorithm without any other changes. For example, we could *adapt* the filter response each time the filter detects a rapid change of the formation transit time via an increase in the error covariance or via a large discrepancy between prediction and measurement. In that case the filter would weight the data a little more for some time, until the discrepancies vanish. As a result, we expect an even better resolution of sharp interfaces without increasing the noise content everywhere on the log. In other words, once we have decided on a given resolution/noise-reduction trade-off, we do not have to stick with it until the inversion is done, as we would in the case of a damped least squares inversion of the whole system.

Role of initial guesses: Steady-state filter

Figures 9A and 9B investigate the consequences of starting the recursion with erroneous guesses in the case of a noise free data set and in a noise corrupted situation respectively. In both situations the filter corrects the error. The only difference is the time it takes to do so. This suggests that, in the long run, the output is totally independent of initial state specifications. In others words, it reaches a steady state. This has very important implications with respect to all practical applications.

Kalman filtering is computationally time consuming. In any case, one could compute and store the gains $K(j)$ and error covariances $P(j \mid j)$ ahead of time.

A steady state would enable the user to apply a constant gain K. The resulting process would no longer be optimal in terms of minimizing the error covariance, but, after some time, it would be very near optimality. The steady state approximation would be a more computationally efficient process to apply and just as quick as any finite response filtering. It would, however, lose the great flexibility and adaptability to data of that type of formulation. Nevertheless, depending on the application sought, one might want to apply a non depth-dependent filter. In this case, the Kalman filter formulation provides us with theoretical results. Based upon the properties of the linear system under consideration, namely its *Observability* and *Controllability*, it is possible to conclude the existence of a steady-state filter. Intuitively, observability means that, when the state equation is taken without input noise, one can retrieve the initial state from an exact observation of the system over a finite period of time. Controllability means that it takes a finite period of time to bring the system to any given state through chosen deterministic inputs. Both properties were verified by the single spacing as well as the multiple spacing systems. Given our choice of a state equation, controllability was always verified. Assuming that the observation is made in such a way as to involve all entries of the state vector at least once, observability is always guaranteed. (This last condition is sufficient but not necessary.) Therefore, we may conclude the existence of a steady-state filter.

Other examples

Figures 10 and 11 display results for three and four layer models respectively, involving thin layers of 5 ft and 2.5 ft thicknesses (note the change of depth scale in Figure 11). In all the cases presented, least squares inverses show a better noise reduction than their conventional counterparts.

It appears that recursive least squares inverses tend to under estimate transit time variations. Moreover, even in the case of a symmetric contrast such as in Figure 10, the inversion does not keep that feature. This is related to the causal nature of the Kalman filter. However, better estimates could be obtained by combining both forward and backward Kalman filters (Smith, 1975).

REAL DATA EXAMPLE

We processed a 150 foot limestone section of arrival time data. The tool configuration is that of Figure 3. Firing rate and logging speed are the same. Figure 12 displays one 10 ft offset arrival time data scaled in $\mu s/ft$. (We had only one of the two 10 ft offset arrival time determination available and we duplicated it with the correct shift of 2 ft).

Figure 13 shows results of the "conventional" processing. Outputs of least squares processings for various statistical specifications are presented in Figures 14, 15 and 16. Each one of these needs about 10 sec of cpu time to complete 50 depth increments on a VAX 11/780 with a non-optimized program. Statistical specifications are kept constant throughout the inversion. The expected formation variability, Q, is 100 for all three figures. The noise variance, R, is 1, 10 and 100 for Figures 14, 15 and 16 respectively.

As for inversions conducted on synthetic data, outputs of conventional and least squares processings are similar for a small value of R (quick Kalman filter case) except for differences in the sharpness and magnitude of some of the picks. The three least squares processings further illustrate the resolution/noise reduction trade off discussed earlier and the need for an adaptive processing. In particular, the moderate resolutions obtained show that resolution is critically limited by the noise content of the data. Each one of these output curves corresponds to different hypotheses concerning the relative importance of the noise content versus the formation variability. Obviously, knowledge of the actual noise content prevents exaggerated smoothing out of the results. Still, even knowing its actual characteristics will not help the filter to discriminate between real formation changes and noise corruption.

CONCLUSIONS

As one can see from these examples, there is a need for a better definition of resolution. Resolving power is usually taken to be the smallest layer thickness one can distinguish in a homogeneous formation. This is also the ability of the output to rise promptly when a step function is input. This is true in noise-free situations. Nevertheless, resolution through noise corrupted data is a more complicated matter as underlined by the few examples presented in this study. Resolving a thin layer is important, but not showing a layer when there is none is also important. This is part of a well known trade-off that occurs in any estimation problem.

Least squares inversion provides us with a reliable way of obtaining reasonable answers to this problem using probabilistic constraints. It takes into account a very general piece of geological information -- the vertical sequentiality of physical parameters. It uses the best of the statistical redundancy that is not used normally in the case of a single spacing tool, and is poorly used in the case of multi-spacing tools.

The Kalman filter formulation makes processing affordable from the standpoint of storage size, and its great flexibility makes it a very powerful and promising approach. However, further work is needed to design an inversion process which would include borehole radius and would also be adaptable to large formation changes.

ACKNOWLEDGEMENTS

I would like to thank Dr. Gilles Garcia for many discussions on this subject as well as for his careful review of this paper. I am indebted to the ELF AQUITAINE company for providing me with the fellowship at M.I.T.

REFERENCES

Foster, M., Hicks, W., and Nipper, J., 1962, Optimum inverse filters which shorten the spacing of velocity logs: Geophysics, 27, 317-326.

O'Doherty, R.F. and Anstey, N.A., 1971, Reflections on Amplitudes: Geophysical Prospecting, 19, 430-458

Sandell Jr., N.R. and Shapiro, J.H., 1976, Stochastic processes and applications, notes for subject 6.432, Department of EECS, Massachusetts Institute of Technology, Cambridge, Massachusetts.

Smith, P.L., 1975, Backward-Forward Smoothing Interpretation of the *A Posteriori* Process Noise Estimate, IEEE Trans. on Automatic Control.

Willis, M.E., 1983, Inversion of travel time for velocity : Annual Report of the Full Waveform Acoustic Logging Consortium, Earth Resources Laboratory, Department of EAPS, Massachusetts Institute of Technology, Cambridge, Massachusetts.

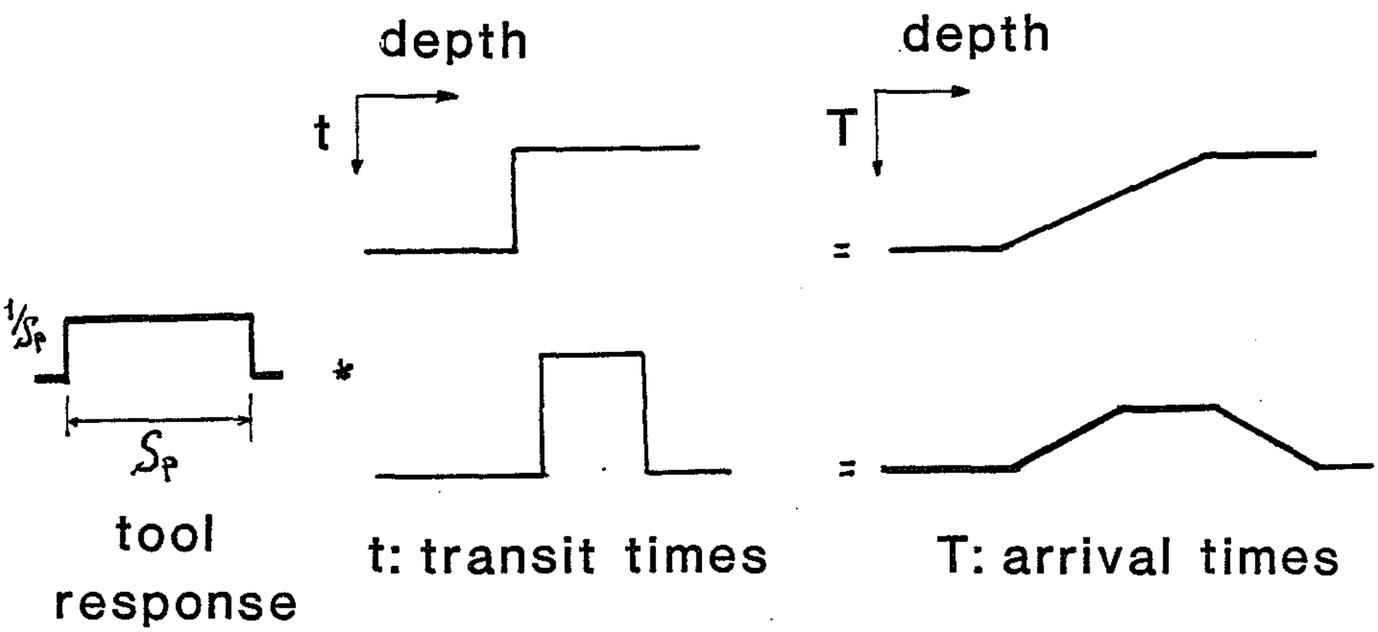

Figure 1 : Smoothing effect of the source-receiver separation on travel times in the cases of a sharp interface and a thin layer.

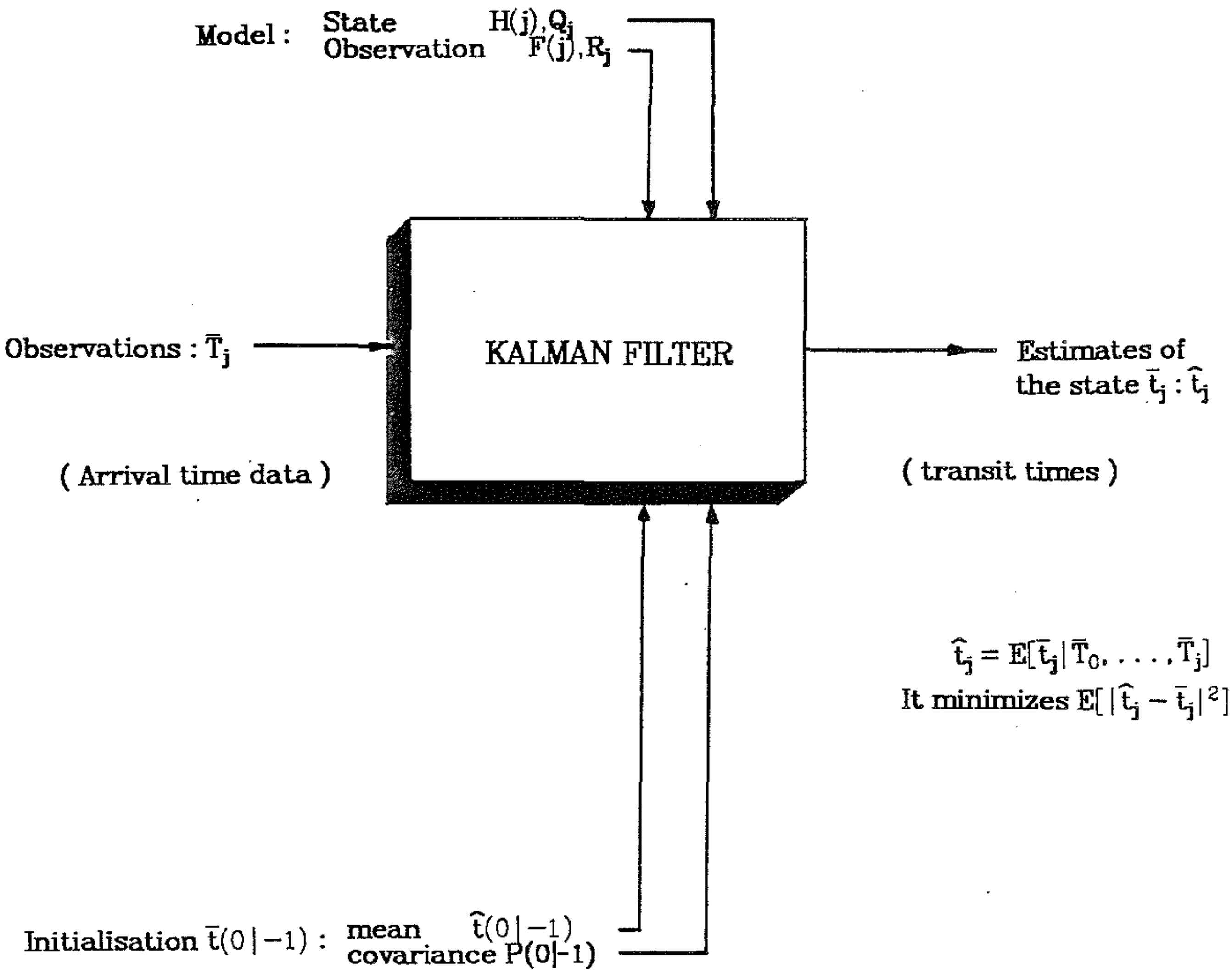

Figure 2 : Summary of the different inputs and initial specifications for Kalman filtering.

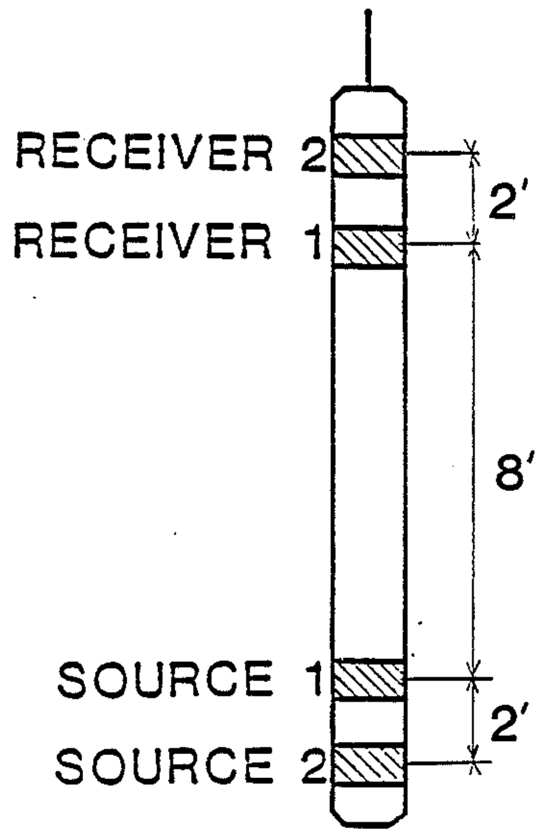

SPACINGS : 10' 8' 12' and 10'

A complete sequence is fired every 1/2'

Figure 3 : Tool geometric configuration used to simulate processing of synthetic data.

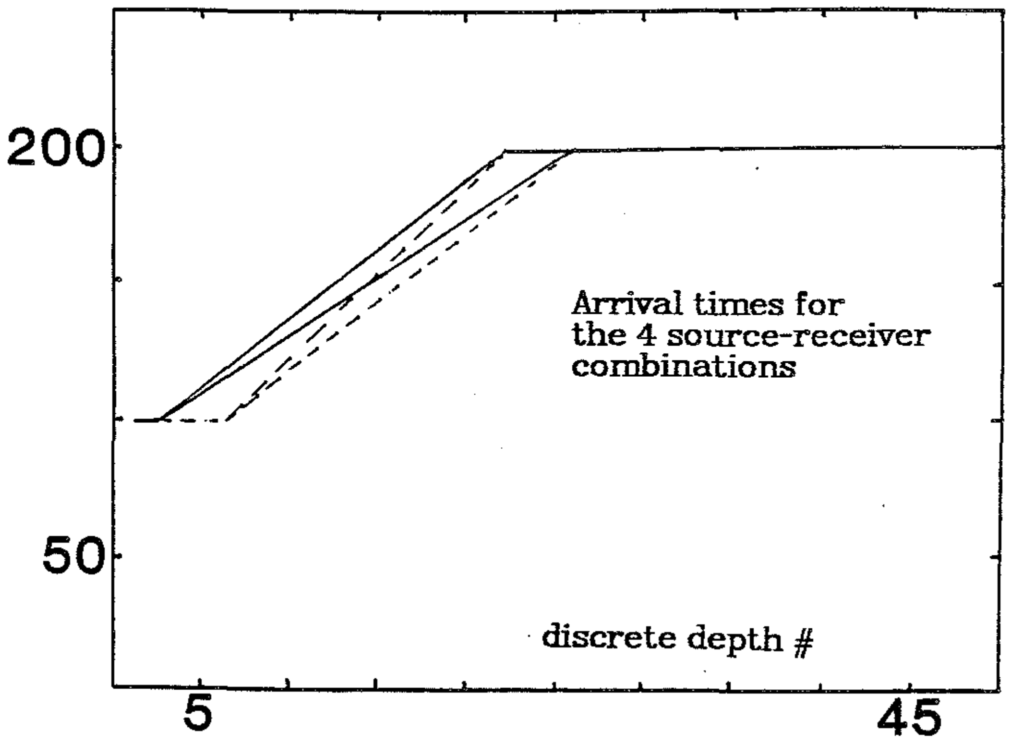

Figure 4 : Synthetic arrival-time curves for the tool of Figure 3 in the case of a sharp interface. Scale units are explained in the text.

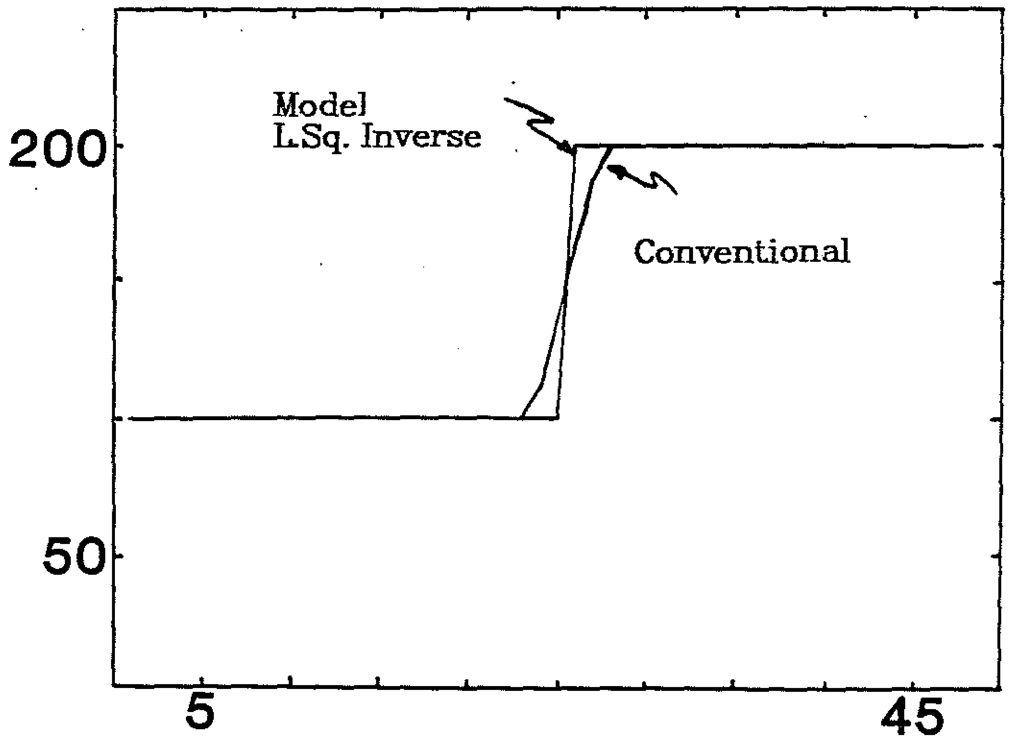

Figure 5 : Outputs of conventional and recursive least squares processing in the case of the noise-free data set of Figure 4.

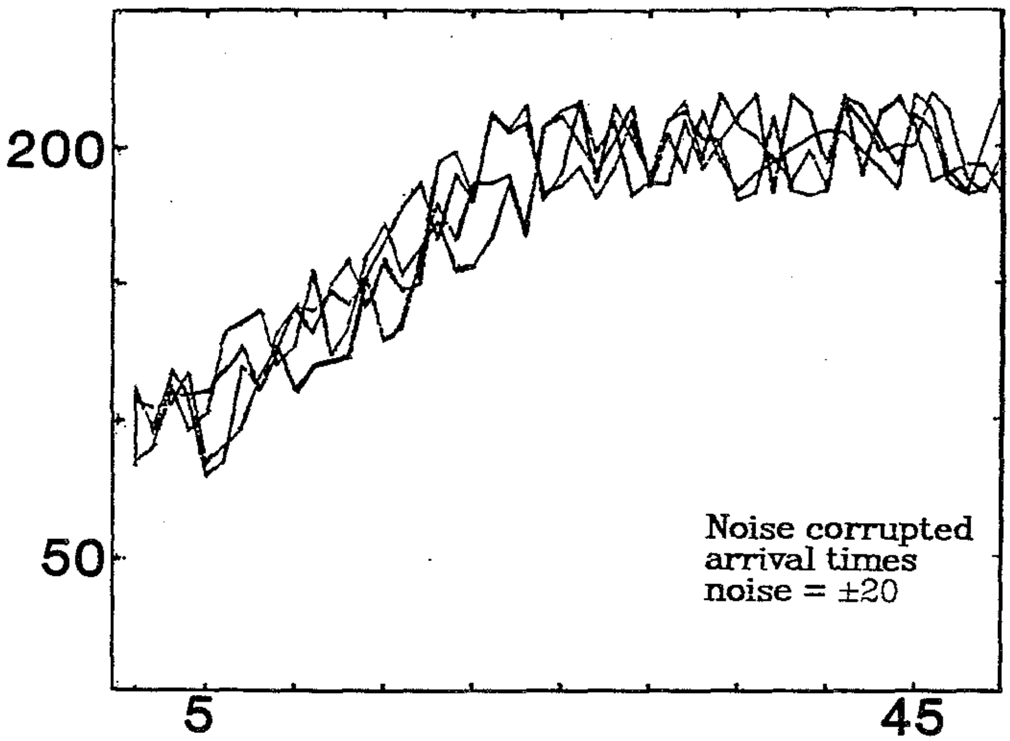

Figure 6 : Synthetic arrival-time curves of Figure 4 have been corrupted by an additive random noise of maximum amplitude 20.

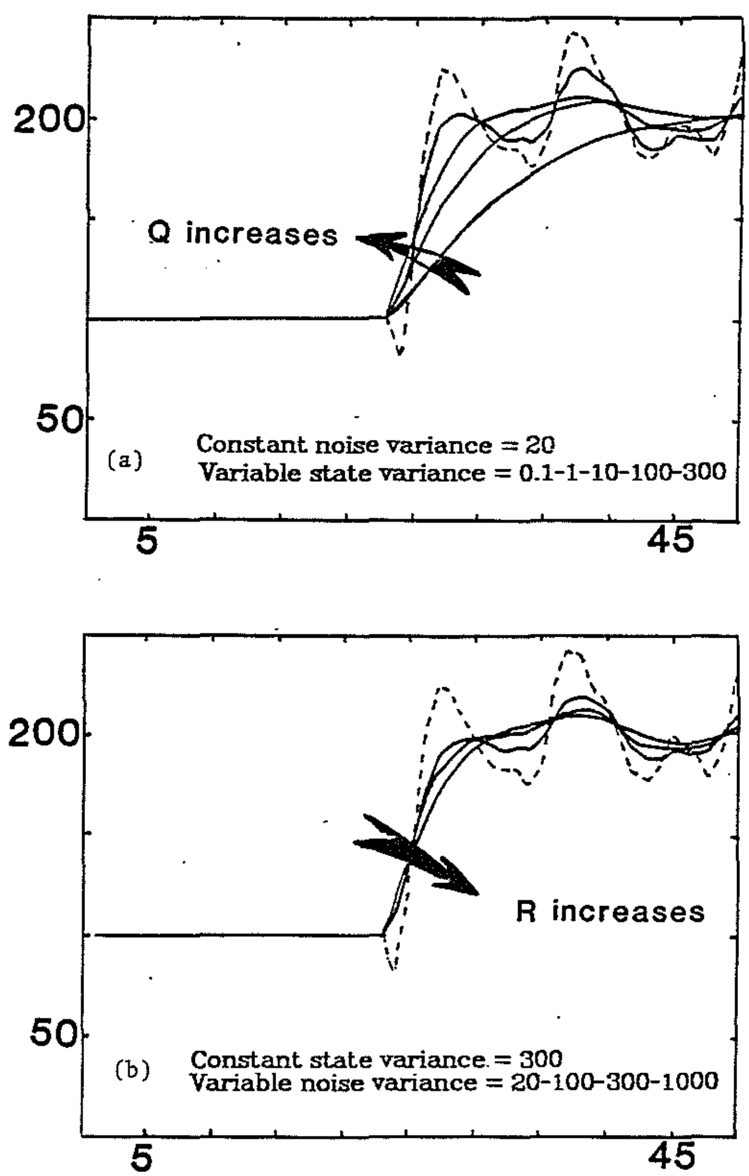

Figure 7A and 7B : Outputs of the recursive least squares processing for various noise specifications (Q and R). A correct initial guess has been assumed.
(A) R, the observation noise variance is kept constant, Q increases
(B) Q, the "expected" formation variability is kept constant, R increases
In both figures, the dashed curve is obtained with the same R and Q.

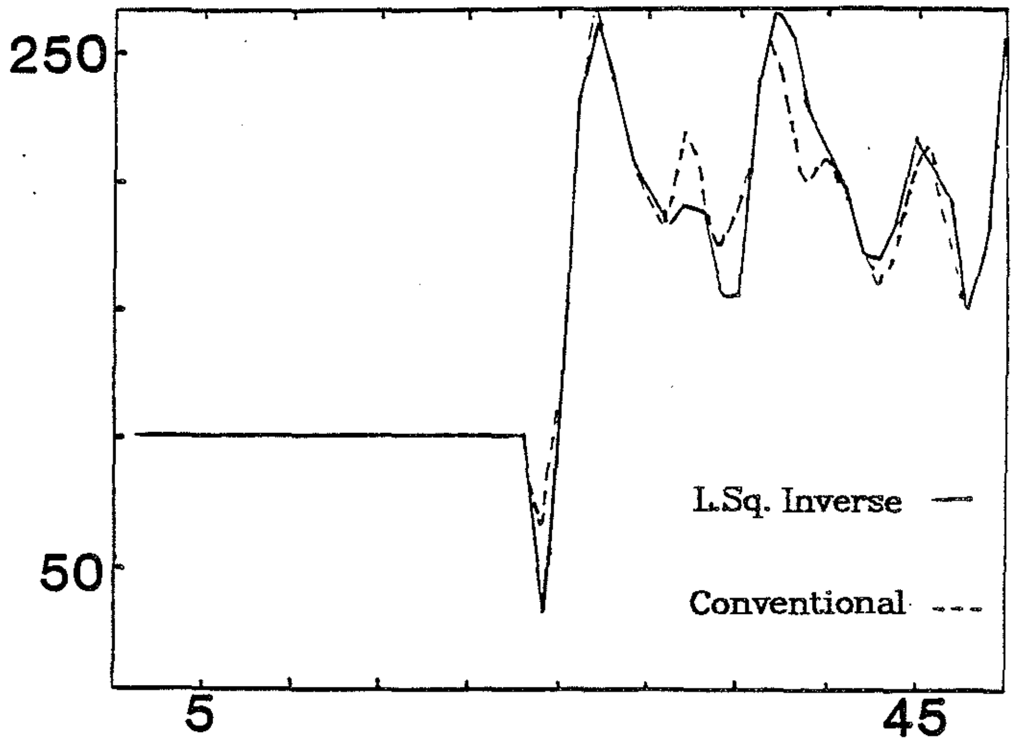

Figure 8 : Outputs of both conventional and quick Kalman processing.

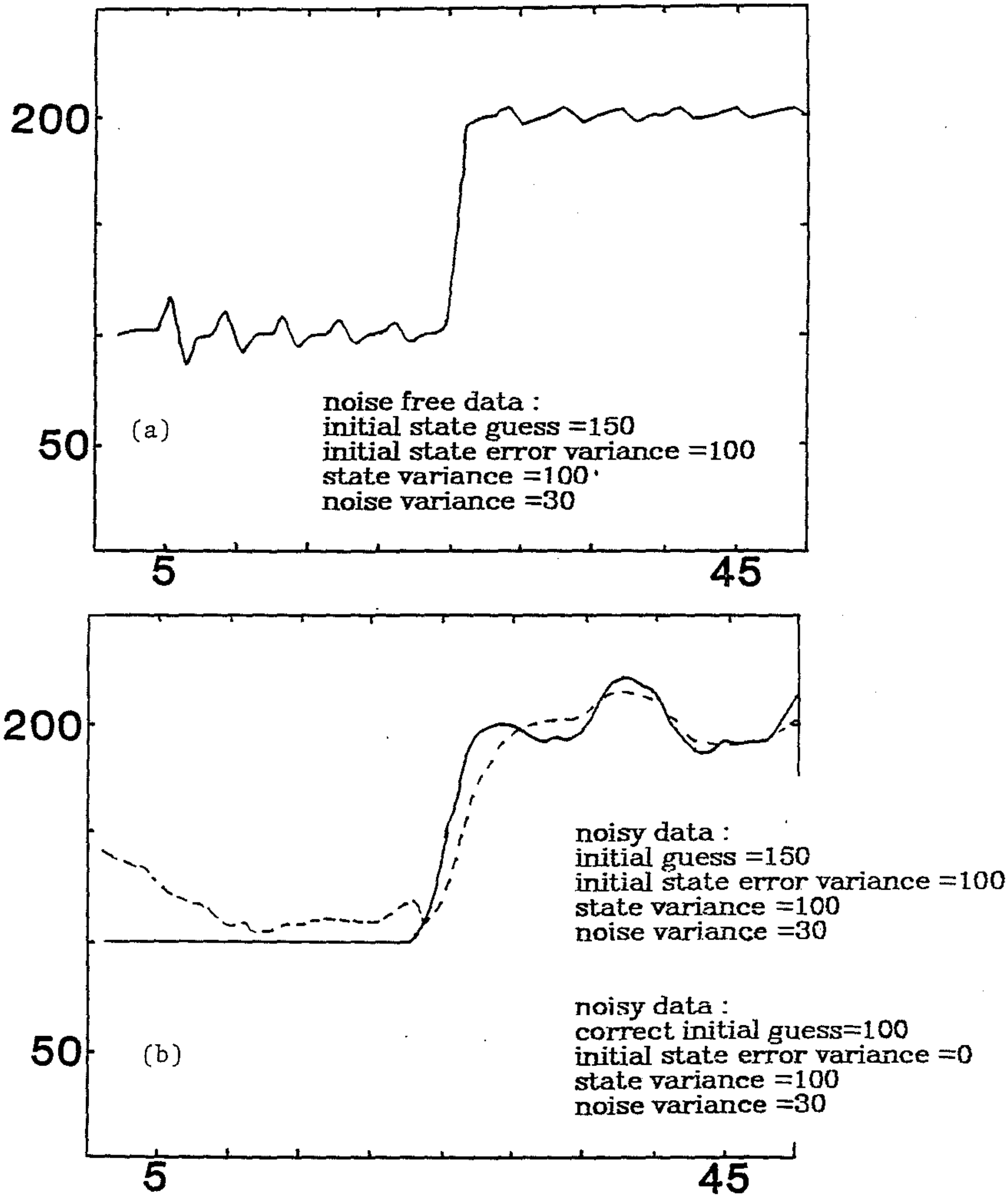

Figure 9A and 9B : Output of recursive least squares processing in the case of erroneous initial guesses.
(A) with the noise-free data set. (B) with the noise-corrupted data set.

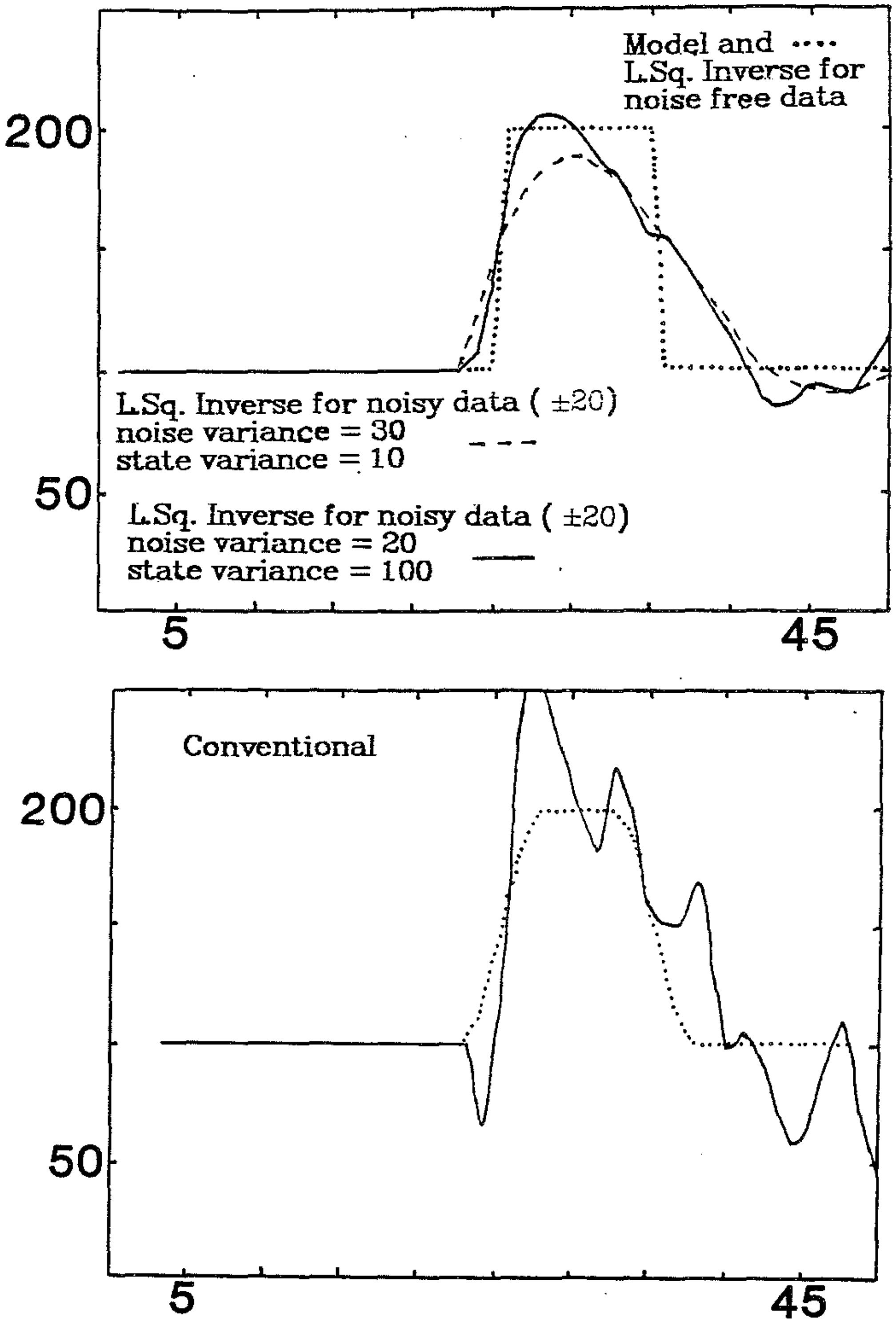

Figure 10 : Results of both conventional and recursive-least squares processing for a three layer model. The medium layer is 5' thick.

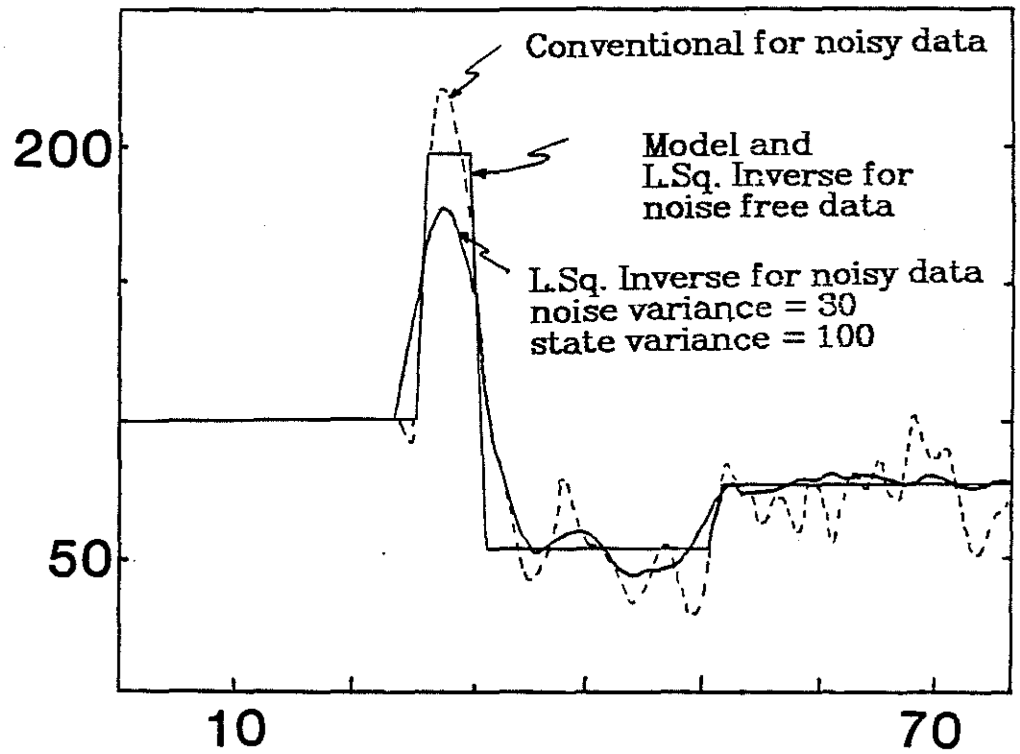

Figure 11 : Results of both conventional and recursive least squares processing for a four layer model. The thinner layer is 2.5' thick.

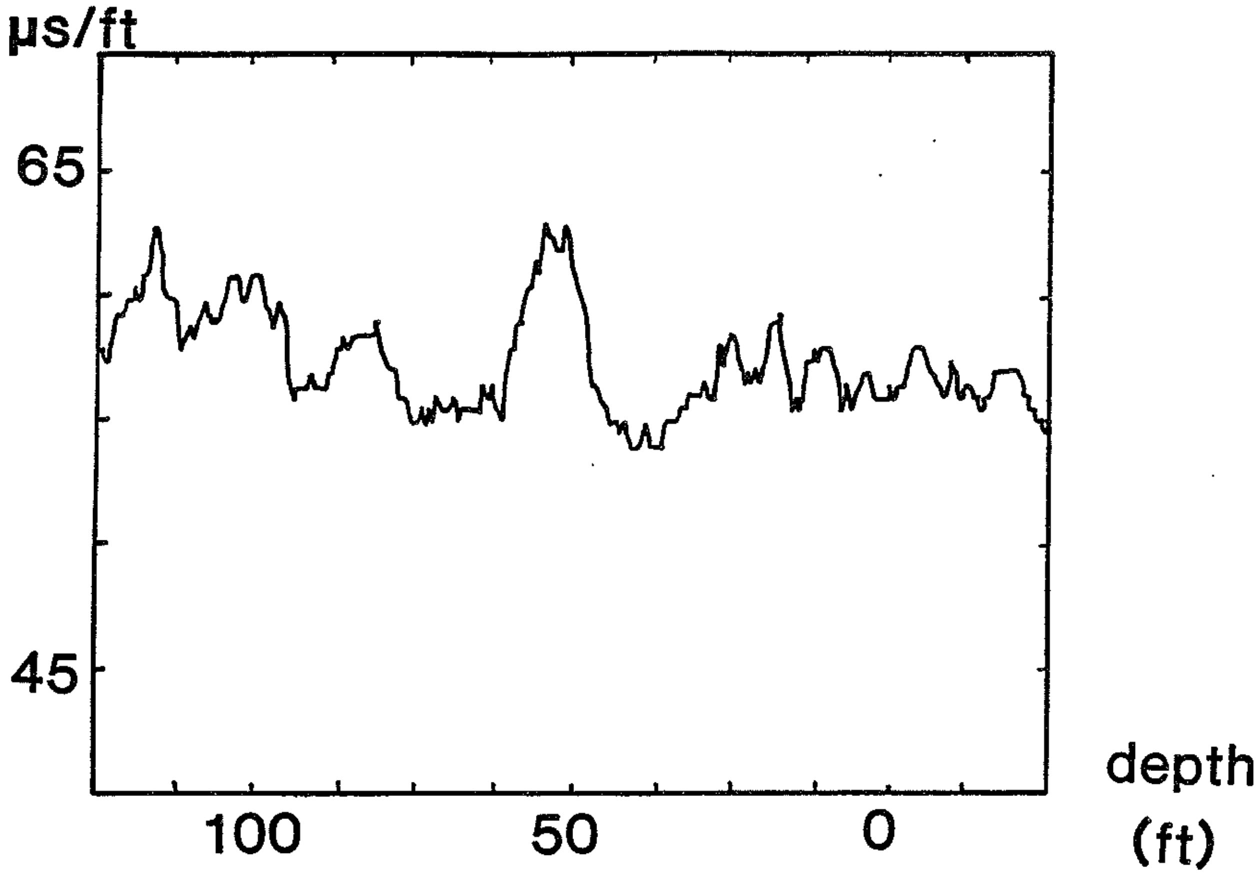

Figure 12 : Arrival time determinations for a 10 foot spacing used as part of the input for the next real data processing examples.

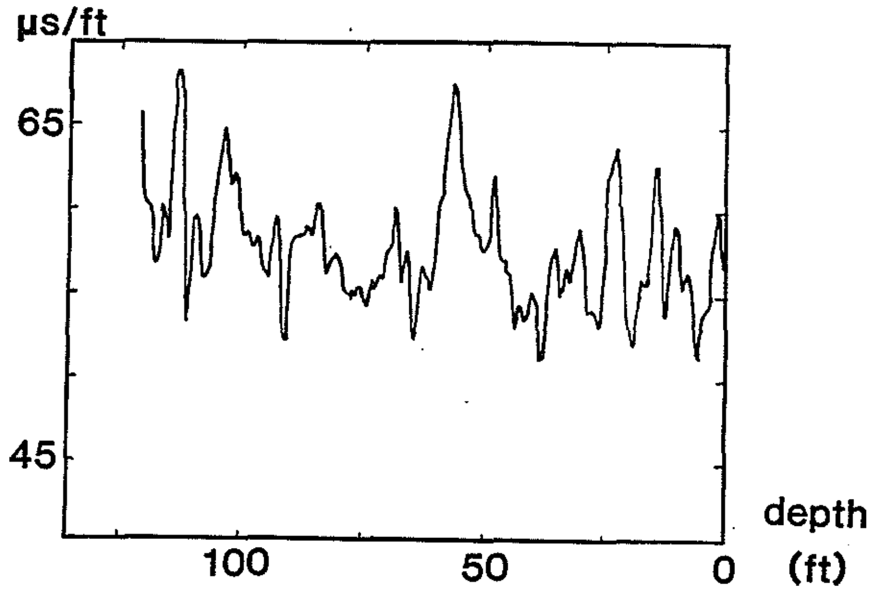

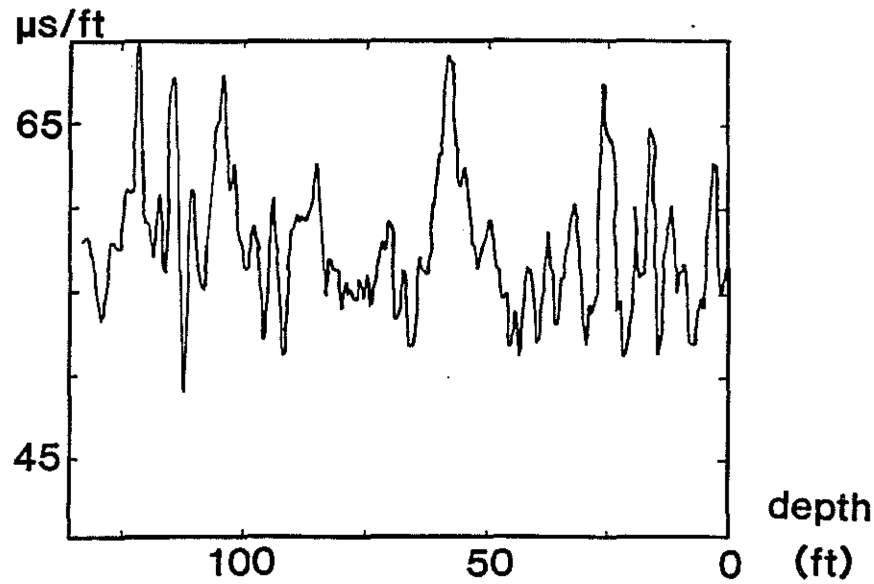

Figure 13 (top) : Conventional processing example on real data

Figure 14 (bottom) : Least squares processing of the real data of Figure 12. Q=100 and R=1.

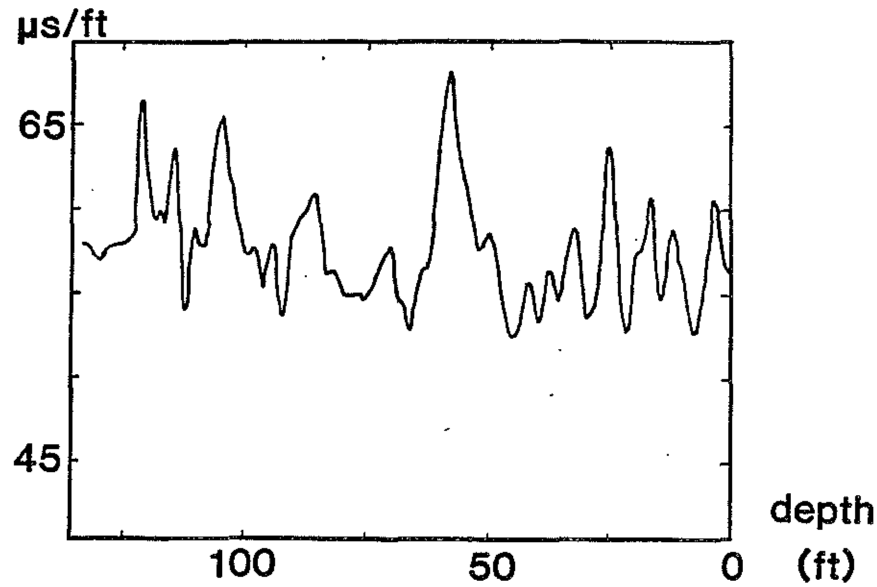

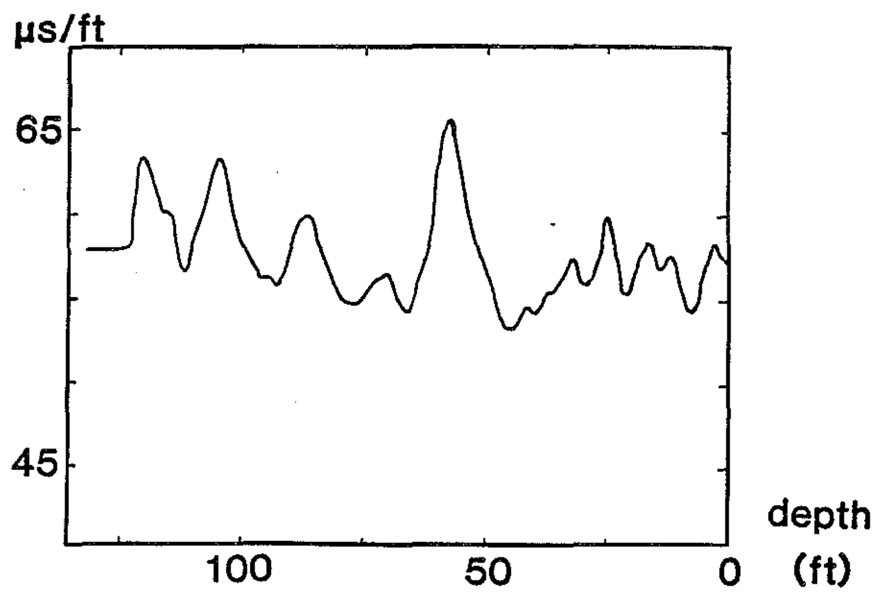

Figure 15 (top) : Least squares processing of the real data of Figure 12. Q=100 and R=10.

Figure 16 (bottom) : Least squares processing of the real data of Figure 12. Q=100 and R=100.